

# Articles

## Preparation and Utilization of Organically Modified Silica–Titania Photocatalysts for Decontamination of Aquatic Environments

Geula Dagan, Srinivasan Sampath, and Ovadia Lev\*

Fredy and Nadine Herrmann School of Applied Science, Division of Environmental Sciences, The Hebrew University of Jerusalem, Jerusalem 91904, Israel

Received March 8, 1994. Revised Manuscript Received October 10, 1994<sup>®</sup>

A new class of photocatalysts that can be used for decontamination of aquatic environments from organic and chloroorganic contaminants is reported. The photocatalysts are comprised of homogeneous dispersion of TiO<sub>2</sub> nanocrystals in organically modified SiO<sub>2</sub>. These composite materials were prepared by a two-step acid catalyzed sol–gel preparation protocol. The combination of the improved photocatalytic activity of homogeneous dispersion of segregated nanocrystalline TiO<sub>2</sub> and the adsorption properties of organically modified silica increases the rate of decomposition of hydrophobic organic pollutants in aquatic environments. An additional advantage of these catalysts is their floating capability. This property provides a possibility of using them under solar illumination. The activity of the organically modified SiO<sub>2</sub>–TiO<sub>2</sub> catalyst is compared with that of commercial nanocrystalline TiO<sub>2</sub> and TiO<sub>2</sub>–SiO<sub>2</sub> and TiO<sub>2</sub> sol–gel derived xerogels, under solar light and UV lamp irradiation.

### Introduction

The theoretical basis of semiconductor-mediated photocatalysis is well established.<sup>1</sup> Highly potent oxidants (holes) can be produced at the semiconductor surface, by illumination of wide-bandgap semiconducting materials (such as TiO<sub>2</sub> and ZnO), using light with higher energy than their bandgap. These energetic species can be used for photocatalytic detoxification of aquatic and gaseous environments. The above mentioned principles have found applications in the field of environmental chemistry and pollution control.<sup>2</sup> The complete photocatalyzed disappearance and, at times, the complete destructive mineralization have been demonstrated for a number of solutes. This includes, for example, halogenated aliphatic<sup>2c,3</sup> and aromatic<sup>2,4</sup> hydrocarbons and nitrogen-containing compounds such as ammonia and cyanides,<sup>5</sup> surfactants,<sup>6a</sup> and several precious and base

metal complexes.<sup>2a</sup>

Anatase, a crystalline form of TiO<sub>2</sub>, is particularly effective for the oxidation of organic<sup>6</sup> and simple inorganic compounds.<sup>5</sup> Solid TiO<sub>2</sub> electrodes have high bulk densities, and they sink in water. They can be used in closed systems equipped with external illumination. However, as long-wavelength UV may be used as the photoexciting light for TiO<sub>2</sub>, the photocatalytic reaction can be solar powered. If solar illumination is to be utilized, solid electrodes can operate only in shallow water (for example, at the bottom of a container). For solar powered applications, it is desirable to use a floating photocatalyst.<sup>7,8</sup> Recent attempts along these lines include the use of commercial TiO<sub>2</sub> (P-25

\* Author for correspondence.

<sup>®</sup> Abstract published in *Advance ACS Abstracts*, November 15, 1994.

(1) (a) *Homogeneous and Heterogeneous Photocatalysis*; Pelizzetti, E., Serpone, N., Eds.; D. Reidel: Dordrecht, The Netherlands, 1985. (b) *Photoelectrochemistry, Photocatalysis and Photoreactors*; Schiavello, M., Ed.; D. Reidel: Dordrecht, The Netherlands, 1985. (c) *Energy Resources through Photochemistry and Catalysis*; Gratzel, M., Ed.; Academic Press: New York, 1983.

(2) For example: (a) Serpone, N.; Pelizzetti, E. *Photocatalysis—Fundamentals and Applications*; Wiley: New York, 1989; Chapter 18, p 603. (b) Kamat, P. V. *Kinetics and Catalysis in Microheterogeneous Systems*; Gratzel, M., Ed.; Marcel Dekker Inc.: New York, 1991. (c) Bahnemann, D.; Bockelmann, D.; Goslich, R. *Sol. Ener. Mater.* **1991**, *24*, 564. (d) Alpert, D. J.; Sprung, J. L.; Pacheco, J. E.; Prairie, M. R.; Reilly, H. E.; Milne, T. A.; Nimlos, M. R. *Sol. Ener. Mater.* **1991**, *24*, 594. (e) Blake, D. M.; Webb, J.; Turchi, C.; Magrini, K. *Sol. Energy Mater.* **1991**, *24*, 584.

(3) (a) Frank, S. N.; Bard, A. J. *J. Phys. Chem.* **1977**, *81*, 1484. (b) Peterson, M. W.; Turner, J. A.; Nozik, A. J. *J. Phys. Chem.* **1991**, *95*, 222. (c) Palmans, R.; Frank, A. J. *J. Phys. Chem.* **1991**, *95*, 9338. (d) Kormann, C.; Bahnemann, D. W.; Hoffmann, M. R. *J. Photochem. Photobiol.* **1989**, *48*, 161. (e) Kormann, C.; Bahnemann, D. W.;

Hoffmann, M. R. *Environ. Sci. Technol.* **1988**, *22*, 798. (f) Tunesi, S.; Anderson, M. A. *J. Phys. Chem.* **1991**, *95*, 3399. (g) Minoura, H.; Katoh, Y.; Sugiura, T.; Ueno, Y.; Matsui, M.; Shibata, K. *Chem. Phys. Lett.* **1990**, *173*, 220.

(4) (a) Fox, M. A. *Res. Chem. Intermediates* **1991**, *15*, 153. (b) Kakuta, N.; Park, K. H.; Finlayson, M. F.; Ueno, A.; Bard, A. J.; Campion, A.; Fox, M. A.; Webber, S. E.; White, J. M. *J. Phys. Chem.* **1985**, *89*, 732. (c) Sakka, S.; Kamiya, K.; Yoko, T. *ACS Symp. Ser. No. 360, Inorganic and Organic Polymers*; Zeldin, M., Wynne, K. J., Allcock, H. R., Eds.; American Chemical Society: Washington, DC, 1988. (d) Sabate, J.; Anderson, M. A.; Kikkawa, H.; Edwards, M.; Hill, C. G., Jr. *J. Catal.* **1991**, *127*, 167. (e) Barbeni, M.; Pramauro, E.; Pelizzetti, E.; Borgarello, E.; Serpone, N.; Jamieson, M. A. *Chemosphere* **1986**, *15*, 1913.

(5) For example: (a) Cant, N. W.; Cole, J. R. *J. Catal.* **1992**, *134*, 317. (b) Hidaka, H.; Nakamura, T.; Ishizaka, A.; Tsuchiya, M.; Shao, J. *J. Photochem. Photobiol. A: Chem.* **1992**, *66*, 367. (c) Mihaylov, B. V.; Hendrix, J. L.; Nelson, J. H. *J. Photochem. Photobiol., A: Chem.* **1993**, *72*, 172.

(6) For example: (a) Hidaka, H.; Zhao, J.; Pelizzetti, E.; Serpone, N. *J. Phys. Chem.* **1992**, *96*, 2226. (b) Vinodgopal, K.; Kamat, P. V. *J. Phys. Chem.* **1992**, *96*, 5053. (c) Matthews, R. W. *J. Phys. Chem.* **1987**, *91*, 3328.

(7) (a) Guillet, J. E.; Sherren, J.; Gharapetian, H. M.; MacInnis, W. K. *J. Photochem.* **1984**, *25*, 501. (b) Jackson, N. B.; Wang, C. M.; Luo, Z.; Schwitzgebel, J.; Ekerdt, J. G.; Brock, J. R.; Heller, A. *J. Electrochem. Soc.* **1991**, *138*, 3660.

Degussa) coated on hollow glass beads<sup>7b</sup> and solid pieces of highly porous TiO<sub>2</sub> aerogels.<sup>8</sup>

Mixed oxides and other composite materials, such as V<sub>2</sub>O<sub>5</sub>/TiO<sub>2</sub>,<sup>9</sup> MoO<sub>3</sub>/TiO<sub>2</sub>,<sup>10</sup> NiO/K<sub>4</sub>Nb<sub>6</sub>O<sub>17</sub>,<sup>11</sup> CrO<sub>3</sub>/SiO<sub>2</sub> (or) Al<sub>2</sub>O<sub>3</sub>,<sup>12</sup> NiO/TiO<sub>2</sub>,<sup>13</sup> SiO<sub>2</sub>/TiO<sub>2</sub>,<sup>14-17</sup> platinumized SiO<sub>2</sub>/TiO<sub>2</sub>,<sup>18,19</sup> MgO/TiO<sub>2</sub>,<sup>17</sup> and several others<sup>20-28</sup> have been reported to be efficient catalysts for various reactions. In some of these cases the mixed oxides are used to optimize the energy bandgap and minimize photocorrosion and in others (e.g., silica- or alumina-titania photocatalysts), the motivation stems from the improved adsorption and concentration of the reactants in the vicinity of the active catalytic centers. The role of the adsorption step in the photocatalytic process has been well studied,<sup>29,30</sup> and the conversion rate was found to depend on the ability to concentrate the target species on the surface of the semiconductor or in its vicinity.<sup>29-31</sup> To improve the degradation rate of hydrophobic compounds that do not adsorb on pure TiO<sub>2</sub>, it is desired to design photocatalysts that will adsorb and concentrate the degradable compounds but will still allow their diffusion from the adsorption site to the vicinity of the electrode. Indeed, titania coated carbon powder was recently shown to exhibit improved photodegradation performance as compared to the performance of pure titania.<sup>32</sup> However, carbon absorbs light, and its surface functional groups form irreversible bonds to many organic pollutants. This low lability may obstruct the

mobility and transport of organic pollutants to the close proximity of the active photocatalytic centers.

The sol-gel technology provides a convenient way to produce mixed oxides, and an opportunity to tailor the chemical and physical properties of inorganic oxides by modifying their preparation conditions. Thus, porous, organically modified ceramics (Ormocers)<sup>33</sup> that are used in this research are prepared, via the sol-gel method, by using precursors containing Si-C bonds such as methyl-, phenyl- and other organotrialkoxysilanes. The Si-C bond does not participate in the hydrolysis and polycondensation steps. The porous surface of the resulting xerogel is covered with organic functional groups (R) that remain exposed at the pore surface. This implies that surface properties, such as cage polarity, hydrophobicity, ion-exchange capacity and the concentration of silanol groups can be modified by changing the type and concentration of -R. Polar and nonpolar regions can be produced on the same material, by preparing a glass of mixed organically modified and nonmodified oxides. Modified sol-gel-derived ceramics (Ormocers) were found to have photometric, chromatographic,<sup>34</sup> and electrochemical applications.<sup>35</sup>

In this study, we introduce, characterize, and demonstrate a new class of photocatalysts, mixed material of organically modified SiO<sub>2</sub> and TiO<sub>2</sub>. These photocatalysts are porous materials containing almost homogeneous distribution of segregated (not clustered) nanocrystals (quantum dot dimension) of TiO<sub>2</sub> imbedded in organically modified SiO<sub>2</sub> backbone. This combination allows for efficient reversible adsorption of target organic compounds, short traveling distance from the adsorbed site to the active centers and higher oxidation capabilities, which stem from the larger bandgap of quantum dot TiO<sub>2</sub> crystals. Additionally, floating catalysts can be prepared by exploiting the water rejection by hydrophobic, organically modified surfaces.

## Experimental Details

**Materials.** The organosilane (tetramethoxysilane, methyltrimethoxysilane, phenyltrimethoxysilane) were purchased from ABCR, Inc. (Karlsruhe, Germany). Titanium isopropoxide was purchased from Aldrich (Milwaukee, WI). Nanocrystalline Degussa P-25 titania powder (ca. 80:20 anatase:rutile ratio) was used for comparative studies due to its high reported activity for degradation of the phenol derivatives.<sup>36,37</sup> Phenol, chlorinated phenols, and salicylic acid were purchased from Sigma (St. Louis, MO) and used without further purification. Unless otherwise specified analytical grade reagents and triply distilled water (resistivity greater than 20 MΩ/cm) were used.

**Apparatus.** Transmission electron microscopy (TEM) was carried out using a JEOL (JEM 200CX) microscope with an operating voltage of 200 kV. X-ray powder diffraction was measured with a Philips automated powder diffractometer (Cu Kα radiation) at 1°/min. scan rate. The concentration of the aromatic substances was measured by a Hewlett-Packard Model 8452A diode array spectrophotometer. The hydrophobicity of the materials was quantitated by measurements of the water contact angle on the flat surface of the photocatalyst.

- (8) (a) Dagan, G.; Tomkiewicz, M. *J. Phys. Chem.* **1993**, *97*, 12651. (b) Dagan, G.; Tomkiewicz, M. In *Environmental Aspects of Electrochemistry and Photoelectrochemistry*, Yoneyama, H., Tomkiewicz, M., Eds.; The Electrochemical Society: Pennington, NJ, 1993.
- (9) Deo, G.; Wachs, I. E. *J. Catal.* **1994**, *146*, 335.
- (10) Martin, C.; Martin, I.; del Moral, C.; Rives, V. *J. Catal.* **1994**, *146*, 415.
- (11) Kudo, A.; Tanaka, A.; Domen, K.; Maruya, K.; Aika, K.; Onishi, T. *J. Catal.* **1988**, *111*, 67.
- (12) De Rossi, S.; Ferraris, G.; Fremiotti, S.; Garrone, E.; Ghiotti, G.; Campa, M. C.; Indivina, V. *J. Catal.* **1994**, *148*, 138.
- (13) Kudo, A.; Domen, K.; Maruya, K.; Onishi, T. *Chem. Phys. Lett.* **1987**, *133*, 517.
- (14) (a) Anpo, M.; Nakaya, H.; Kodama, S.; Kubokawa, Y.; Domen, K.; Onishi, T. *J. Phys. Chem.* **1986**, *90*, 1633. (b) Anpo, M.; Aikawa, N.; Kubokawa, Y.; Che, M.; Louis, C.; Giamello, E. *J. Phys. Chem.* **1985**, *89*, 5017.
- (15) Frank, A. J.; Willner, I.; Goren, Z.; Degani, Y. *J. Am. Chem. Soc.* **1987**, *109*, 3568.
- (16) Rao, K. V.; Rama Rao, M.; Nair, M. P.; Kumar, V. G.; Nair, C. G. R. *Int. J. Hydrogen Energy* **1989**, *14*, 295.
- (17) Palmisano, L.; Schiavello, M.; Sclafani, A.; Coluccia, S.; Marchese, L. *New J. Chem.* **1988**, *12*, 847.
- (18) Enea, O.; Ali, A. *New J. Chem.* **1988**, *12*, 853.
- (19) (a) Domen, K.; Sakata, Y.; Kudo, A.; Maruya, K.; Onishi, T. *Bull. Chem. Soc. Jpn.* **1988**, *61*, 359. (b) Kodama, S.; Nakaya, H.; Anpo, M.; Kubokawa, Y. *Bull. Chem. Soc. Jpn.* **1985**, *58*, 3645.
- (20) Krenske, D.; Abdo, S.; Van Damme, H.; Cruz, M.; Fripiat, J. *J. Phys. Chem.* **1980**, *84*, 2447.
- (21) Suib, S. L.; Tanguay, J. F.; Ocelli, M. L. *J. Am. Chem. Soc.* **1986**, *108*, 6972.
- (22) Enea, O.; Bard, A. J. *J. Phys. Chem.* **1986**, *90*, 301.
- (23) Villemure, G.; Kodama, H.; Detellier, C. *Can. J. Chem.* **1985**, *63*, 1139.
- (24) Krishnan, M.; White, J. M.; Fox, M. A.; Bard, A. J. *J. Am. Chem. Soc.* **1983**, *105*, 1983.
- (25) Nijs, H.; Fripiat, J. J.; Van Damme, H. *J. Phys. Chem.* **1983**, *87*, 1279.
- (26) DellaGuardia, R. A.; Thomas, J. K. *J. Phys. Chem.* **1983**, *87*, 990.
- (27) Abdo, S.; Canesson, P.; Cruz, M.; Fripiat, J. J.; Van Damme, H. *J. Phys. Chem.* **1981**, *85*, 797.
- (28) Ueno, A.; Kakuta, N.; Park, K. H.; Finlayson, M. F.; Bard, J.; Campion, A.; Fox, M. A.; Webber, S. E.; White, J. M. *J. Phys. Chem.* **1985**, *89*, 3828.
- (29) Minero, C.; Catozzo, F.; Pelizzetti, E. *Langmuir* **1992**, *8*, 481.
- (30) Kormann, C.; Bahnemann, D. W.; Hoffmann, M. R. *Environ. Sci. Technol.* **1991**, *25*, 494.
- (31) (a) Turchi, C. S.; Ollis, D. F. *J. Phys. Chem.* **1988**, *92*, 6852. (b) Matthews, R. W. *J. Phys. Chem.* **1988**, *92*, 6853. (c) Turchi, C. S.; Ollis, D. F. *J. Catal.* **1990**, *122*, 178.
- (32) Uchida, H.; Itoh, S.; Yoneyama, H. *Chem. Lett.* **1993**, 1995.

- (33) (a) Philipp, G.; Schmidt, H. *J. Non-Cryst. Solids* **1984**, *63*, 283. (b) Schmidt, H. *J. Non-Cryst. Solids* **1990**, *121*, 428.
- (34) (a) Tsionsky, M.; Lev, O. *Analyst* **1993**, *118*, 557. (b) Kuselman, I.; Lev, O. *Talanta* **1993**, *40*, 749. (c) Glezer, V.; Lev, O. *J. Am. Chem. Soc.* **1993**, *115*, 2533. (d) Lev, O. *Analyst* **1992**, *20*, 543.
- (35) (a) Tsionsky, M.; Gun, G.; Glezer, V.; Lev, O. *Anal. Chem.* **1994**, *66*, 1747. (b) Gun, G.; Tsionsky, M.; Lev, O. *Anal. Chim. Acta* **1994**, *294*, 261.
- (36) Al-Ekabi, H.; Serpone, N. *J. Phys. Chem.* **1988**, *92*, 5726.
- (37) Matthews, R. W. *J. Phys. Chem.* **1987**, *91*, 3328.

This was carried out using Rame-Hart Inc., NRL C.A., Goniometer Model No. 100-00230. Adsorption isotherms were obtained using an ASAP 2000 (Micromeritics) instrument.

**Preparation of Composite Photocatalysts.** Ormocers-TiO<sub>2</sub> gels were prepared by a two-stage acid-catalyzed sol-gel method. Because of the difference in the hydrolyzation rates of alkoxy silanes and titanium tetraisopropoxide, the sols were prepared separately and mixed at the last stage. Organically modified silica sols were prepared by mixing the precursor (R-Si(OCH<sub>3</sub>)<sub>3</sub>; R = methyl or phenyl) with ethanol and 0.1 M HCl at 40–50 °C with stirring for 2 h. The molar ratio between R-Si(OCH<sub>3</sub>)<sub>3</sub>:ethanol:H<sub>2</sub>O was 1:5:3. Titania sol was prepared by mixing Ti(IV) isopropoxide with ethanol and 0.1 M HCl, in a water-ice bath with 15 min of stirring. The molar ratio between Ti(IV) isopropoxide:ethanol:H<sub>2</sub>O was 1:20:3. The silica and titania sols were mixed and stirred for 1/2 h before molding. Gelation was completed within several days. The gels were allowed to age at room temperature for at least twice the gelation time and, subsequently, at 42 °C for 5 h. To remove residues of the unreacted materials, the catalyst was washed for about 12 h with water, ethanol mixture (1:1 by volume). The two-step preparation procedure of the Ormocers was essential for obtaining a homogeneous photocatalyst. A one-step preparation protocol yielded segregated precipitates of titanium oxide.

Mixed oxides of SiO<sub>2</sub>-TiO<sub>2</sub> (nonmodified silica), with the same ratio between silica and titania as for the modified silica-based materials, were prepared by the same procedure, using Si(OCH<sub>3</sub>)<sub>4</sub> as the Si precursor. These nonmodified mixed oxides together with TiO<sub>2</sub> xerogels served as reference compounds in the study of photocatalytic activity of the (modified) silica-titania xerogels. TiO<sub>2</sub> xerogels were prepared as was reported previously.<sup>8</sup> The photocatalytic activity of these materials was also compared with that of commercial TiO<sub>2</sub> powder (Degussa, P-25). The use of this TiO<sub>2</sub> powder in many other photodegradation studies (e.g., refs 2c, 3, 4c, and 29) makes it a suitable reference material.

**Material Characterization.** Surface area was determined by multipoint Brunauer-Emmett-Teller (BET) measurements.<sup>38</sup> The samples were preheated overnight at 60 °C before the measurement. Total pore volume ( $V_{TP}$ ), was obtained from the N<sub>2</sub> adsorption isotherm at a partial pressure of 0.99. Bulk densities ( $d_b$ ) were obtained from the weight/volume of monolithic pieces. The results represent an average over three or four measurements, which agree within an error range of 10% or less.

**Preparation of Samples for TEM.** Mixed modified silica and titania sol (Si:Ti = 1:0.2) was prepared according to the above-mentioned procedure. After the mixed sol was stirred for about 30 min, a portion of it was diluted with ethanol. A drop of the sol was then placed on thin copper grids (G400, Polaron equipment Ltd., Watford, England), and the solvent was evaporated simultaneously allowing the gelation to complete. The TEM studies were conducted several days after the preparation.

**Photodegradation Studies.** The extensive use of aromatic halocarbons in industries makes them appropriate candidates for photodegradation experiments. Phenol and substituted phenols were used as model contaminants in this study. Stock solutions of 1 and 3 mM phenol, 0.7, 1.75, and 3.5 mM 4-chlorophenol in 1 mM NaCl were prepared. The initial concentration of 2,4-dichlorophenol, 3,4-dichlorophenol and salicylic acid was 1 mM in 1 mM aqueous NaCl. In each experiment, 25 mL of the contaminant solution was added to 0.5 g of the photocatalyst and left to equilibrate in the dark. The amount of pure TiO<sub>2</sub> catalyst used was the same as that of the TiO<sub>2</sub> component in the mixed oxide catalysts.

Photodecomposition experiments were performed using crushed catalysts, with and without stirring in an open Pyrex cell illuminated from above. The cell was irradiated by a mercury lamp equipped with a 300 nm cutoff filter. The output of the lamp showed characteristic peaks at 313 and 365 nm. The intensity (in the 280–390 range) as measured using a (Ophir, Model 30A) power meter was 1.0 mW/cm<sup>2</sup>. Solar

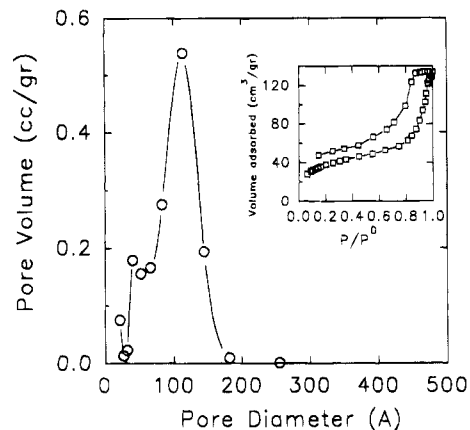


**Figure 1.** Pore size distribution, calculated from the desorption isotherm and plotted as  $dV_p/d \log R_p$  vs  $D_p$  ( $V_p$ , pore volume in cm<sup>3</sup>/g;  $D_p$ , pore diameter in angstroms) for sample A1. Inset: The adsorption-desorption isotherms of nitrogen at 77 K of sample A1.

**Table 1. Composition, Wetting Angle, and Bulk Density ( $d_b$ , g/cm<sup>3</sup>) of the Xerogels Used in This Study**

sample	R	SiO <sub>2</sub> :TiO <sub>2</sub>	wetting angle	$d_b$
A1	methyl	1:0.05	104	1.19
A2	phenyl	1:0.05	103	1.24
A3		1:0.05		1.62
B1	methyl	1:0.10	107	1.15
B2	phenyl	1:0.10	100	0.94
B3		1:0.10		1.57
C	methyl	1:0.14	103	1.15
D	methyl	1:0.20	103	1.10
F	methyl	1:0.40	105	1.25
TiO <sub>2</sub> xerogel		0:1		1.55

irradiation intensity between 295 and 385 nm was measured by an Eppley UV radiometer (Photometer) and is given in Figure 8b. Solar intensity was monitored every 1 min and averaged over every hour.

**Adsorption Studies.** Adsorption of phenol and 4-chlorophenol on different photocatalysts was studied at the same experimental conditions (concentrations, pH, ionic strength, temperature) as for the photodegradation studies. These experiments were performed in the dark to avoid photooxidation. The concentrations of the organic molecules were obtained from the peak absorbance of the different compounds. The wavelengths of absorbance measurements for different compounds are 270 nm for phenol, 280 nm for 4-chlorophenol, 284 nm for 3,4-dichlorophenol, 296 nm for salicylic acid, and 290 nm for 2,4-dichlorophenol.

## Results and Discussion

**Characterization of the Photocatalysts.** A series of gels, with different SiO<sub>2</sub>-TiO<sub>2</sub> ratios and with either methyl or phenyl as the functional group, were prepared. Xerogels of TiO<sub>2</sub>, SiO<sub>2</sub>-TiO<sub>2</sub> (nonmodified silica), and Degussa P-25 powder were used as reference compounds for the photocatalytic activity of the modified silica-titania xerogels. The compositions of the gels prepared for this study are shown in Table 1. The numbers represent the molar ratio between Si and Ti in the reaction mixture.

Pore size distribution for sample A1, as calculated from the desorption part of the isotherm, is shown in Figure 1. The material contains pores of diameter in the range 35–170 Å and the average is 78 Å. The inset in Figure 1 shows the adsorption-desorption isotherms of this sample. For most of the organically modified samples, nitrogen adsorption isotherms indicate a very low surface area. The open hysteresis shown in Figure 1 was observed for the other Ormocers as well. Such

(38) Gregg, S. J.; Sing, K. S. W. *Adsorption, Surface Area and Porosity*; Academic Press: New York, 1982; Chapter 3.

**Table 2. BET Surface area (m<sup>2</sup>/g), Total Pore Volume (TPV, cm<sup>3</sup>/g) and Average Pore Diameter (D<sub>p</sub>, Å) for Xerogels Used in This Study**

sample	BET (m <sup>2</sup> /g)	TPV (cm <sup>3</sup> /g)	D <sub>p</sub> (Å)
A1	140	0.2	78
A2	<2	nd	nd
A3	<2	nd	nd
B1	51	0.043	40
B2	<2	nd	nd
B3	836	0.4	25
C	<2	nd	490
D	<2	nd	280
F	<2	nd	nd
TiO <sub>2</sub> xerogel	141	0.16	35 <sup>b</sup>
TiO <sub>2</sub> Degussa <sup>a</sup>	54	0.063	

<sup>a</sup> The manufacturer's data. <sup>b</sup> nd: The porosity is comprised of micropores and macropores for which the nitrogen adsorption technique is inadequate.



**Figure 2.** Floating pieces of sample F (CH<sub>3</sub>-SiO<sub>2</sub>:TiO<sub>2</sub>, ratio 1:0.4), on water.

behavior is characteristic of microporous xerogels, which are often produced by acid-catalyzed sol-gel process.<sup>39</sup> CO<sub>2</sub> adsorption isotherms were found to reveal additional unaccounted for, microporous surface area,<sup>39</sup> which, however, is inaccessible for catalysis. Table 2 summarizes the morphological characteristics of these materials.

The phenyl- and methyl-modified ceramics exhibit hydrophobic external surfaces. Water was rejected and only the external surface and a microdimension deep layer near it was wetted. Table 1 reveals that in all cases the water contact angles were above 90°. Despite the rough surface, these values are indicative of the surface hydrophobicity of organically modified materials. This property, in addition to the relatively low bulk density of the Ormocers, which was in some cases lower than the specific density of water, yield improved buoyancy. Solid pieces and powders can float on water for periods that can last from several days to more than several months. Figure 2 illustrates the floating capability of large monoliths containing 40% TiO<sub>2</sub> (sample F). Indeed, this phenomenon reduces the active surface

**Table 3. Freundlich Adsorption Constants for 4-Chlorophenol on Photocatalysts Used in This Study**

sample	K (mg/g)(L/mg) <sup>1/n</sup>	1/n
B	11.9 × 10 <sup>-2</sup>	2.42
F	3.6	0.61
B3	2.0 × 10 <sup>-2</sup>	1.4
Degussa	3.4 × 10 <sup>-4</sup>	2.5

of the catalysts since the internal surface does not contribute to the photocatalyses, but the improved adsorption of the hydrophobic surface and the good floatation can compensate for this drawback.

**Crystallinity.** X-ray powder diffraction did not reveal the crystallinity of the modified or that of the nonmodified SiO<sub>2</sub>-TiO<sub>2</sub>, prepared by the two-step procedure (Figure 3B). However, transmission electron microscopy studies showed the presence of segregated nanocrystalline TiO<sub>2</sub> particles which were uniformly distributed over the silica matrix (Figure 3A). The crystallinity of TiO<sub>2</sub> was confirmed by electron diffraction (not shown). The size of the titania particles were less than 4 nm. Quantum confinement effects start to increase the photocatalyst bandgap when the size of the titania crystals becomes less than approximately 4 nm (e.g., the bandgap is increased from 3.2 to 4 eV by decreasing the particle size from 4 to 1 nm).<sup>40</sup> Thus, quantum-sized particles can effect good photodegradation by producing holes of very high oxidizing power.

**Adsorption Studies.** The adsorption isotherms on the various photocatalysts were studied. The time dependence of adsorption of 4-chlorophenol (initial concentration 1.75 mM) on modified SiO<sub>2</sub>-TiO<sub>2</sub> xerogels (samples B1 and F) as compared to pure TiO<sub>2</sub> xerogel, are shown in Figure 4. Figure 5 shows adsorption profiles of 4-chlorophenol (concentration on the solid vs the initial solution concentration) on samples B1 and F, as compared to nonmodified SiO<sub>2</sub>-TiO<sub>2</sub> and to commercial (Degussa) powder. The inset of Figure 5 shows the corresponding Freundlich adsorption isotherms. Freundlich constants, K and 1/n were calculated according to the eq 1 and are presented in Table 3:

$$\log q_e = \log K + (1/n) \log C_e \quad (1)$$

where  $q_e$  and  $C_e$  are the equilibrium surface and solution concentrations, respectively. It is clear from Figures 4 and 5 (and similar results that were obtained for adsorption of phenol) that adsorption of hydrophobic materials on organically modified mixed oxides is much better than on nonmodified oxides (SiO<sub>2</sub>-TiO<sub>2</sub>, and pure TiO<sub>2</sub>). Despite the fact that only the outer surface of the organically modified material is active, its internal surface, which accounts for most of the surface area is inaccessible for water. The difference between the adsorption on the various Ormocers may be attributed to their different microstructure and the composition of the external surface rather than to changes in the total surface area, which remained largely unwetted.

**Photodegradation Studies.** Figure 6 shows photodegradation profiles of 4-chlorophenol on Ormocers-TiO<sub>2</sub> xerogels (samples B2 and C), nonmodified SiO<sub>2</sub>-TiO<sub>2</sub> xerogel (sample B3) and the pure TiO<sub>2</sub> xerogel, as compared to the illuminated solution without the use of a photocatalyst. The ordinate axis depicts the solu-

(39) Samual, J.; Polivaya, Y.; Ottolenghi, M.; Avnir, D. *Chem. Mater.*, in press.

(40) Miyazaki, S.; Yoneyama, H. *Denki Kagaku* 1988, 58, 37.

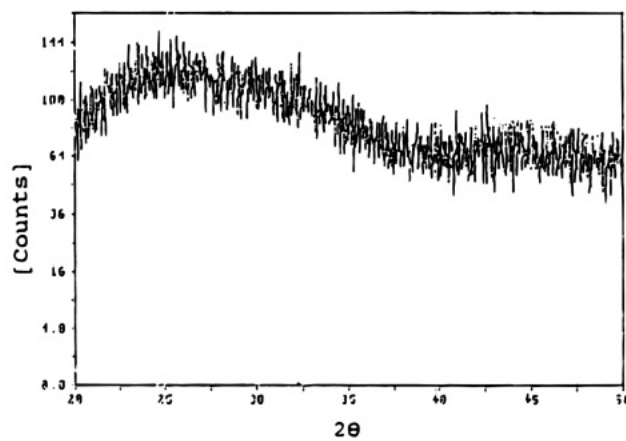
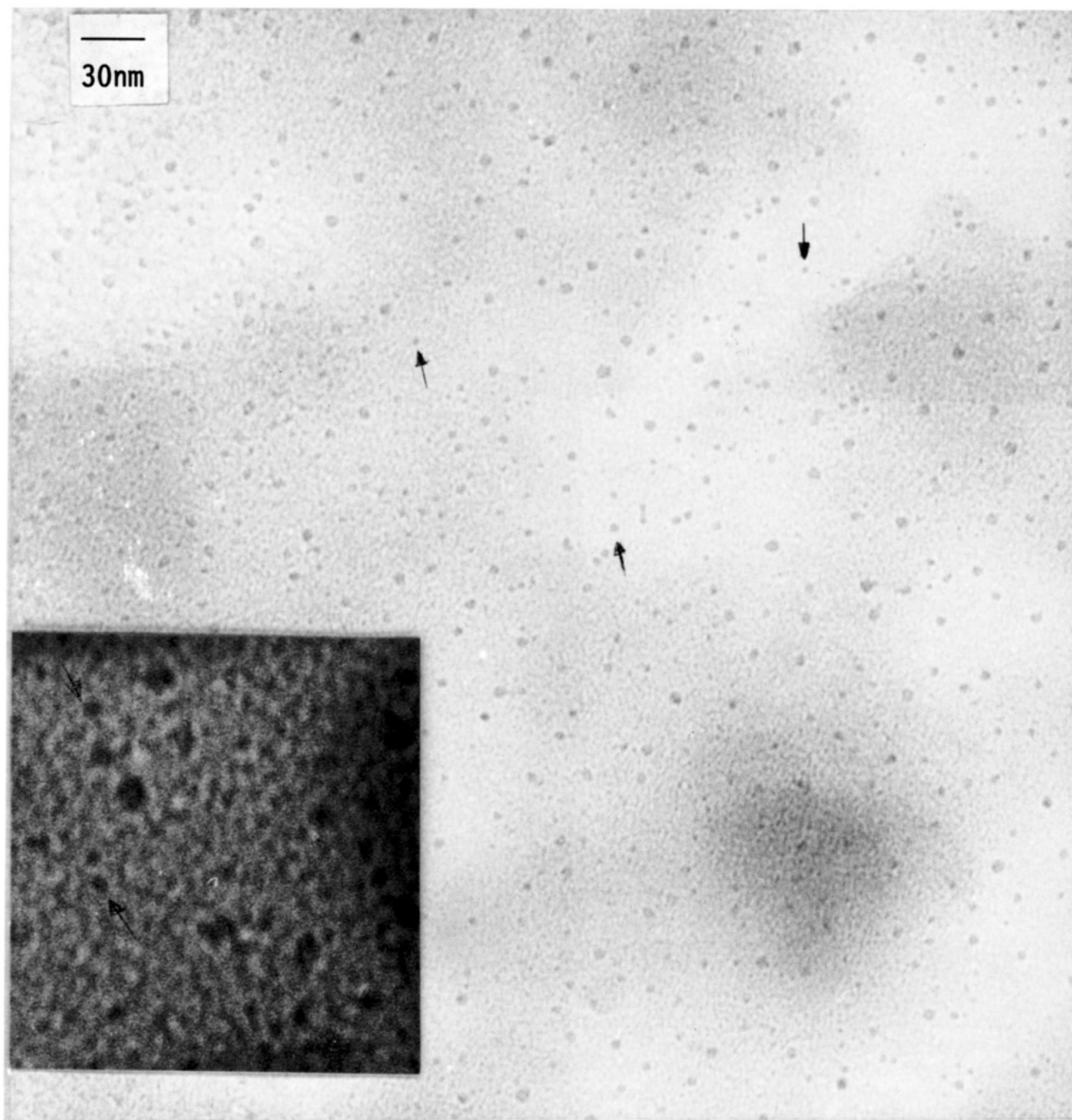


**Figure 3.** (a) TEM picture of methyl-modified SiO<sub>2</sub>-TiO<sub>2</sub>, (Si:Ti ratio 1:0.1). The arrows show crystalline titania particles of various sizes. The operating voltage was 200 kV. The inset was enlarged 7.5 times. (b) Featureless powder X-ray diffraction of the Ormocer-titania sample.



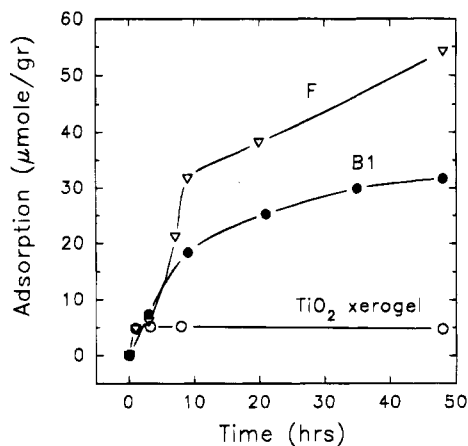


**Figure 4.** Time dependence of adsorption of 4-chlorophenol (presented as micromole of adsorbent on 1 g of catalyst) on modified  $\text{SiO}_2$ - $\text{TiO}_2$  xerogels (samples B1 and F) and on  $\text{TiO}_2$  xerogel. Initial concentration of 4-chlorophenol is 1.75 mM.

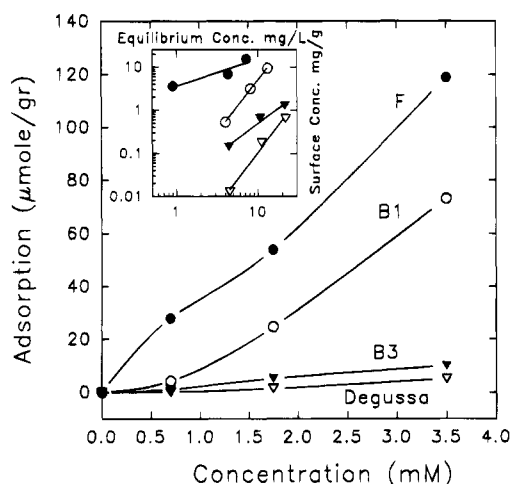


**Figure 5.** Adsorption isotherms of 4-chlorophenol (presented as micromole of adsorbent on 1 g of catalyst) on modified  $\text{SiO}_2$ - $\text{TiO}_2$  xerogels (samples B1 and F), on nonmodified  $\text{SiO}_2$ - $\text{TiO}_2$  (sample B3) and on commercial (Degussa, P-25) powder. Initial concentration of 4-chlorophenol is 1.75 mM. Inset: Freundlich adsorption isotherms (surface concentration vs solution equilibrium concentration) obtained from the same data.

tion concentration of 4-chlorophenol, after illumination for the specific time interval and equilibration. It is clear that direct photodegradation of chlorophenol (and also of phenol) in the absence of photocatalyst does not take place under these experimental conditions (the  $\approx 10\%$  increase in concentration is due to evaporation of the water). It is also observed that photodegradation using Ormocer- $\text{TiO}_2$  xerogels is much faster compared to the nonmodified  $\text{SiO}_2$ - $\text{TiO}_2$  xerogel and the  $\text{TiO}_2$  xerogel.

Figure 7 demonstrates photodegradation profiles of phenol for the modified samples A1, A2, and C as compared to the nonmodified sample B3. It is observed that although the content of the photoactive component  $\text{TiO}_2$  in sample B3 is twice that of samples A1 and A2, photoactivity is much lower in the nonmodified glass. Increasing  $\text{TiO}_2$  content increases the photodegradation rate, in the case of ormocers. In all cases, under solar radiation, as well as under UV lamp irradiation, the photocatalytic activity of the composite Ormocers was much higher than that of the inorganic silica-titania and pure titania xerogels.

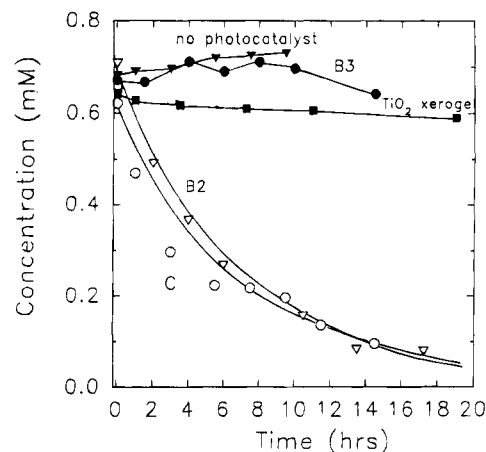


**Figure 6.** Photodegradation profiles of 4-chlorophenol using Ormocer- $\text{TiO}_2$  xerogels (samples B2 and C), nonmodified  $\text{SiO}_2$ - $\text{TiO}_2$  xerogel (sample B3),  $\text{TiO}_2$  xerogel as compared to the illuminated solution without a photocatalyst. Initial concentration of 4-chlorophenol is 0.7 mM. The pH of the contaminant solution was 5.5. The UV illumination intensity was  $1 \text{ mW/cm}^2$ .

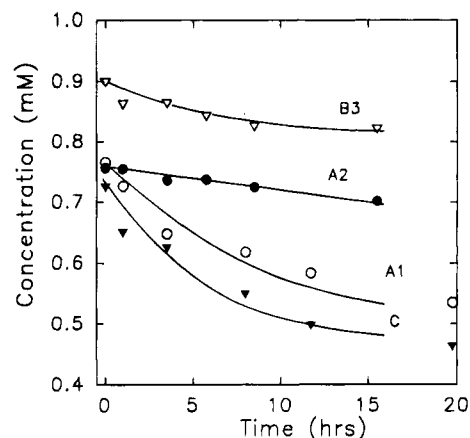


**Figure 7.** Photodegradation profiles of phenol on the Ormocer- $\text{TiO}_2$  xerogels (samples A1, A2, and C) as compared to the  $\text{SiO}_2$ - $\text{TiO}_2$  sample B3. Initial concentration of phenol is 1 mM. Solution pH 5.5. UV intensity  $1 \text{ mW/cm}^2$ .

A comparison of the photodegradation characteristics of phenol and several phenolic derivatives on commercial  $\text{TiO}_2$  (P-25, Degussa) catalyst and B1 composite material is given in Table 4. Several soluble chlorinated phenols were examined along with salicylic acid, which has a similar structure and comparable photodegradation rate on titania,<sup>37</sup> but its basic form shows low affinity to methyl-modified silica. Note, that at pH = 5.5 the salicylate ion is the dominant species ( $\text{p}K_{a,1} = 2.97$ ;  $\text{p}K_{a,2} = 13.4$ ), while all the chlorinated phenols are predominantly in their acidic, molecular forms. The experiments were carried out in 5 cm deep, transparent (for the  $>300 \text{ nm}$  wavelength) beakers, which ensured that even materials that sank to the bottom of the container were still exposed to sunlight. Except for the salicylic acid, the overall removal of the contaminants by the organically modified catalyst was always higher than the commercial material, despite the fact that its exposed surface area was much smaller and its particle size much larger. Moreover, the illuminated cross section of the Ormocer particles was somewhat smaller, since thermal and wind induced turbulence, dispersed the P-25 particles and increased their light exposure, while the floating photocatalysts remained bound to the gas-liquid interface. A conservative estimate of the net

**Table 4. Photodegradation of Organic Compounds over Methyl-Modified SiO<sub>2</sub>-TiO<sub>2</sub> (Catalyst B1) and P-25 Degussa TiO<sub>2</sub> under Solar Irradiation<sup>a</sup>**

compound	initial concn (mM)	B1 catalyst				P-25 TiO <sub>2</sub> catalyst			
		concn after dark equilibration (mM)		concn after 5 h solar photodegradation (mM)		concn after dark equilibration (mM)		concn after 5 h solar photodegradation (mM)	
		I	II	III	IV	V	VI	VII	VIII
phenol	1	0.76	0.77	0.62	0.53	0.98	1.00	0.70	0.22
<i>p</i> -chlorophenol	1	0.70	0.77	0.53	0.56	0.99	0.90	0.70	0.46
2,4-dichlorophenol	1	0.55	0.52	0.22	0.13	0.65	0.63	0.31	<0.05
3,4-dichlorophenol	1	0.83	0.89	0.70	0.40	1.00	1.00	0.90	<0.05
salicylic acid	1	0.94	0.94	0.92	0.92	0.92	0.88	0.77	0.05

<sup>a</sup> II, IV, VI, and VIII are under stirred conditions. Degradation was carried out under solar irradiation on the 28th of June 1994 at Jerusalem. The maximum UV intensity (between 300 and 400 nm) was measured to be 4 mW/cm<sup>2</sup>. The maximum temperature at noon was 35 °C. The pH of the solutions (at the beginning) was 5.5.

photodegradation, which assumes that all the adsorbed species remained undegraded shows only two cases (2,4-dichlorophenol and 3,4-dichlorophenol) for which the performance of the modified photocatalyst was equal or superior to that of the commercial material. The case of the salicylic acid is most revealing, here, adsorption and preconcentration were negligible (and in fact even lower when compared with pure titania, see Table 4, columns I and V) and the photocatalyst performance was considerably inferior to the commercial titania. This again points on the importance of the preconcentration step in the mechanism of photodegradation of organic pollutants by composite Ormocers.

The photodegradation experiments were repeated in stirred solutions. The irradiated cross-section area of the commercial titania was increased, and the external resistance to mass transport decreased, which improved the photoconversion of all the target compounds. Similar stirring had only a minor effect on the photodegradation performance of the organically modified photocatalysts. A pronounced improvement was demonstrated only for 3,4-dichlorophenol which did not adsorb well on the modified catalyst. These observations can be explained by a combination of two facts: (1) The exposed cross section of the organically modified electrode was not increased by stirring, since the catalyst remained confined to the liquid-air interface. (2) When there is a large uptake of the contaminant by the photocatalyst, the internal mass transport to the vicinity of the photoactive center becomes the rate-determining step and thus changes in the external diffusion layer had only little effect on the reaction rate. This, indeed, explains why stirring had the same effect on the photodegradation of 3,4-dichlorophenol on P-25 Degussa TiO<sub>2</sub> and the composite Ormocer. The salicylate which was not adsorbed at all and the well-adsorbed chlorophenols were less affected by the degree of agitation. The complicated photodegradation mechanism is indeed responsible for the clear deviation of the degradation rate from first- or zero-order kinetics.

To check the stability of these materials under UV illumination, we irradiated the photocatalyst, under the same conditions that were used for the activity measurements. The photocatalysts did not lose their hydrophobicity, even after 10 h of illumination with near-UV light or after several days of exposure to sunlight. Figure 8 demonstrates the catalytic stability of the organically modified catalysts after successive photodegradation cycles. The experiments were carried out under solar radiation in June/July (34–35 °C) and the corresponding UV intensity is shown in Figure 8B. The maximum intensity is around 4 mW/cm<sup>2</sup> and is higher

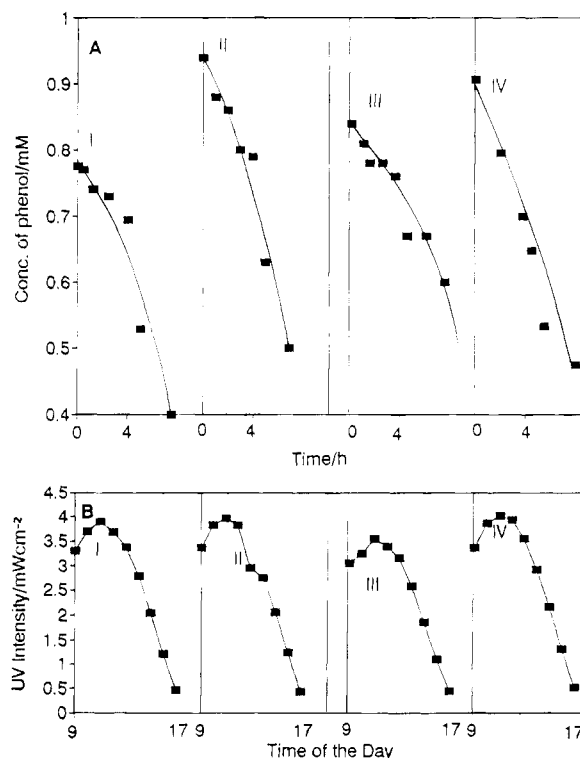


**Figure 8.** (a) Stability of the organically modified SiO<sub>2</sub>-TiO<sub>2</sub> (ratio 1:0.1) as shown by the photodegradation of phenol (concentration 1 mM) under solar irradiation. The irradiation was carried out in June/July at Jerusalem (35 °C). I, II are the first two cycles; III, IV after exposure of the catalyst to sunlight for 10 days. (b) Solar UV intensity on the days of photodegradation tests (from 9 AM to 5 PM).

than the intensity of the lamp used in the simulated experiments. The reaction beaker was spiked with 1 mM phenol, allowed to photodegrade under solar radiation for 8 h, and then the residual concentration of phenol was determined and additional phenol was added to ca. 1 mM. The cycle was repeated four times (only the first and second cycles are depicted in Figure 8) with only small deterioration in the observed photo-reactivity. A second portion of the catalyst was exposed, in aqueous solution, for 10 consecutive days to solar irradiation and then was submitted to similar two test cycles (Figure 8III, IV). Figure 8 demonstrates the high stability of the catalyst under these conditions.

Two basic mechanisms may be responsible for the improved photocatalytic activity of the composite Ormocers. The first involves adsorption of the organic molecule on an adsorption site and migration of the molecule to an adjacent photoactive center (followed by hole formation, heterogeneous charge transfer, and desorption of the intermediates or end products). The

second involves adsorption of the compound on an adsorption site in close proximity to the active center and generation of short-lived radicals that can migrate and oxidize the adsorbed molecules. Figure 3a reveals that the titania particles are uniformly distributed on the silica matrix, leaving an average travelling distance of 7 nm<sup>41</sup> between an adsorption site and the nearest titania crystal. Hence, neither of the two possibilities can be ruled out. The elucidation of relative contribution of each of the reaction pathways is beyond the scope of this paper. However, the inherent properties of Ormocers, as demonstrated above, promote each of the two degradation pathways. The good dispersion of the titania and the homogeneous distribution of the hydrophobic adsorption sites provide the required intimacy for efficient utilization of the short-lived radicals. The labile, hydrophobic interaction of the target molecule with the methyl-modified surface facilitates rapid migration and site exchange of the reactant.

### Conclusions

A new class of photocatalysts based on modified silica-titania composite material was introduced, and its characteristics were demonstrated. Composite Ormocer photocatalysts enjoy the inherent versatility of the sol-gel process, which include, for example, the ability to control the micromorphology of the photocatalyst (including pore size distribution and surface fractal dimension), the ability to produce different configurations (including powders, monoliths, membranes and ceramic coating on glass or other supports), and the favorable optical properties.

Ormocers can be used in order to design desirable surface properties of the photocatalyst by selection of

an appropriate surface modifier from the large variety of commercially available organoalkoxysilane and organochlorosilane compounds. In particular, alkyl-modified silica-titania materials, which were demonstrated in this research, exhibit high affinity to hydrophobic contaminants, reversible bonding of the contaminant and good photodegradation stability under UV and solar radiation.

The materials that were demonstrated here exhibit a homogeneous distribution of segregated titania nanoparticles. Typical dimension of the titania crystals that was demonstrated here is less than 4 nm. This yields two favorable characteristics: (1) The average traveling distance between an adsorption site and a photoactive center is reduced, provided that the titania dots are homogeneously distributed (as demonstrated in Figure 3) and that they are segregated and do not form clusters. (2) The quantum confinement effects which start to play a significant role, increase the bandgap and hence the oxidation potential of the oxidizing holes.

In addition, composite Ormocers can be used as floating catalysts. Hydrophobic composite silica-titania, with low specific bulk density can be produced and since the hydrophobic surface repels water the material does not sink.

**Acknowledgment.** We are grateful to D. Avnir for useful discussions and for facilitating the BET measurements, I. Mayer for X-ray powder diffraction, and to S. Shuraky for the measurements of the solar radiation intensity. The financial supports of the Vallazi-Pikowsky Fund and of the Bundesministerium für Forschung und Technologie, KFK, Karlsruhe, Germany, are gratefully acknowledged.

CM940137M

(41) The average traveling distance was calculated by  $(0.5\sqrt{2})$  (average distance between particles).